



Sustainable production of 5-hydroxymethyl furfural from glucose for process integration with high fructose corn syrup infrastructure

Journal:	<i>Green Chemistry</i>
Manuscript ID	GC-ART-01-2021-000311.R1
Article Type:	Paper
Date Submitted by the Author:	14-Mar-2021
Complete List of Authors:	<p>Chang, Hochan; University of Wisconsin Madison, Chemical and Biological Engineering Bajaj, Ishan; University of Wisconsin Madison, Chemical and Biological Engineering Motagamwala, Ali Hussain; University of Wisconsin-Madison, Chemical and Biological Engineering Somasundaram, Arun; University of Wisconsin-Madison, Chemical and Biological Engineering Huber, George; University of Wisconsin, Chemical and Biological Engineering Maravelias, Christos; Princeton University, Chemical and Biological Engineering Dumesic, James; University of Wisconsin Madison, Chemical and Biological Engineering</p>

ARTICLE

Sustainable production of 5-hydroxymethyl furfural from glucose for process integration with high fructose corn syrup infrastructure

Hochan Chang^{a‡}, Ishan Bajaj^{a‡}, Ali Hussain Motagamwala^a, Arun Somasundaram^a, George W. Huber^a, Christos T. Maravelias^{b,c}, James A. Dumesic^{a,b*}

5-hydroxymethyl furfural (HMF) is a platform chemical, which can be derived from lignocellulosic biomass, and used for production of liquid fuels and polymers. We demonstrate a process for production of HMF using sequential enzymatic and catalytic reactions of glucose to synthesize HMF, and simulated-moving-bed (SMB) separation to purify HMF. The adsorption thermodynamic parameters of glucose, fructose, and HMF on a commercial chromatography resin are experimentally determined for modeling the SMB-based HMF production process. The experimental data are used to develop a rigorous process model and then estimate the cost of production. Chromatographic separation of HMF has 16% lower operating costs compared to an extraction-based process and has a minimum selling price of approximately \$1478 per ton. We demonstrate that the HMF process can be integrated with the high fructose corn syrup (HFCS) process, and we performed analyses considering two systems including construction of a new integrated facility and retrofitting an existing HFCS facility to produce HMF. Our analyses suggest that the latter approach is a promising short-term low-risk strategy to advance the HMF production technology to commercial scale.

Received 00th January 20xx,
Accepted 00th January 20xx

DOI: 10.1039/x0xx00000x

^a Department of Chemical and Biological Engineering, University of Wisconsin–Madison, Madison, WI, USA.

^b DOE Great Lakes Bioenergy Research Center, University of Wisconsin–Madison, Madison, WI, USA.

^c Department of Chemical and Biological Engineering, Princeton University, Princeton, NJ, USA.

[‡]Both authors contributed equally, *Corresponding author E-mail: jdumesic@wisc.edu
Electronic Supplementary Information (ESI) available: [details of any supplementary information available should be included here]. See DOI: 10.1039/x0xx00000x

Introduction

5-hydroxymethyl furfural (HMF) is a widely studied biomass-based platform chemical that has been used to produce liquid fuels and bio-based polymers. Hydrodeoxygenation of HMF over CuRu catalyst can be employed to produce a mixture of branched hydrocarbons and aromatic compounds, which can be used as gasoline additive¹. Diesel and jet fuel can be produced by aldol condensation of HMF to increase the carbon chain, followed by hydrodeoxygenation²⁻⁴. HMF can also be converted into 1,6-hexanediol and tetrahydrofuran dimethanol (THFMD) which are both α - ω diols that can be used to produce polyesters and other polymers⁵. Oxidation of HMF can be carried out to produce an α - ω diacid, 2,5-furan dicarboxylic acid (FDCA)⁶, a monomer used in the synthesis of poly(ethylene furanoate) and poly(butylene furanoate)⁷. The polarity of furan ring in these monomers has been shown to be replacements for PET that have improved barrier properties⁸. Aldol condensation of HMF and acetone has been used for synthesizing a new platform chemical that can be used as an organic dye or monomers⁹.

A large body of research has been performed to address the chemical and technological challenges for production of HMF from biomass resources¹⁰. For instance, glucose¹¹ and fructose¹² can be dehydrated to produce HMF at 60% and 90% yield, respectively, in ionic liquid over an acid catalyst. Fructose was converted to HMF with 90% selectivity at 95% fructose conversion in organic solvent mixtures^{13,14}. However, the use of expensive and toxic solvents (e.g., ionic liquids, organic solvent) negatively affected the process design. Glucose has been utilized as a feedstock due to its inexpensive market price and wide availability. Glucose is an widely available feed, but the unreacted glucose feed must be separated from HMF to produce high purity HMF for applications because the experimental yields of HMF from glucose are limited to be around 50-60%¹⁵. Therefore, glucose is firstly converted to fructose, either by isomerization over an immobilized enzyme¹⁶ or over heterogeneous catalysts, such as Sn- β ¹⁷, followed by dehydration for production of HMF¹⁸.

AVA Biochem developed a commercial scale (20 tons per year) process for production of HMF by using hydrothermal carbonization and purifying HMF by crystallization. However, crystallization of HMF in aqueous solution, which is performed to produce high purity HMF, requires a large energy input to operate refrigeration, and degradation of HMF during the aqueous dehydration reduces the production rate of HMF. Accordingly, development of catalytic reactions with an effective strategy for separating HMF from unreacted sugars and solvents has been a key challenge for production of HMF from sugar resources since HMF degrades in presence of acid catalyst via condensation¹⁹ and is also thermally unstable¹⁹. An organic/aqueous bi-phasic solvent system was used to simultaneously produce and separate HMF²⁰. Excess amounts of salt, such as NaCl, were added to the aqueous phase to maximize HMF partitioning to the organic phase, but the use of salt leads to equipment corrosion and high separation costs. HMF was produced in high yield (63%) from glucose in an acetone/water mono-phasic solvent system, and the separation was achieved by HMF extraction in methyl isobutyl ketone (MIBK) solvent¹⁸. While

extraction is an effective separation technique to isolate pure HMF from the solvent and unreacted sugars, vacuum evaporation and refrigeration were required to separate MIBK from HMF. Moreover, MIBK is an expensive solvent which further increases the operating costs of the process. Chromatographic separation can be an alternative technique that minimizes the operating costs of the process by reducing the refrigeration cost and eliminating the use of additional solvents, like MIBK. Moving-bed chromatographic separation is widely used in industry to purify high fructose corn syrup²¹ and *p*-xylene from xylenes mixtures²².

In this paper, we develop a process based on sequential enzymatic isomerization and catalytic dehydration to produce HMF from glucose in a green co-solvent (acetone/water mixture), followed by chromatographic separation to purify HMF. The solubilities of glucose and fructose in an acetone/water solvent were examined to utilize a maximum concentration of glucose feed at the upper solubility limit. The first step in the process is isomerization of glucose into fructose by using an immobilized glucose isomerase (from *Streptomyces murinus*), in an acetone/water solvent system. The isomerized solution, containing fructose and glucose, is then dehydrated to produce HMF over a solid acid-catalyst, Amberlyst-15. Reaction conditions for dehydration were determined to maximize the HMF yield. Single column chromatography was used to separate HMF from the mixture of the unreacted glucose and fructose. DOWEX 99 Ca/320 resin was used as a stationary phase in chromatography since it is commercially used to separate glucose and fructose for the production of high fructose corn syrup at industrial scale²³. Experiments were performed to determine the adsorption parameters for the adsorption of glucose, fructose, and HMF on the resin. The adsorption parameters were used to optimize simulated-moving-bed (SMB) separation. Using the experimental data, a process model was developed, and a techno-economic analysis (TEA) was performed. TEA suggested that the proposed approach resulted in lower operating cost compared to a MIBK extraction-based process¹⁸ and the process becomes more cost competitive with increase in plant scale. The minimum selling price (MSP) of HMF was computed to be \$1478 per ton for a facility processing 2000 kg·h⁻¹ glucose and producing 8.74 kton of HMF annually. We demonstrate that the proposed process can be integrated with a high fructose corn syrup (HFCS) process to allow sugar producers more flexibility in their product streams. We also develop a process model and perform TEA for the integrated process. Analyses are performed for two systems that include building a new HFCS/HMF facility (greenfield) and retrofitting an existing HFCS facility with an HMF production section (brownfield). The proposed process can be combined with bio-refineries that produce glucose from biomass^{24,25}, and/or embed HMF upgrading process²⁶.

Experimental method

Materials

The following materials were used as received: D-glucose (>99.5%, Sigma-Aldrich), D-fructose (>99%, Fisher chemical), D-cellobiose (>98%, Sigma-Aldrich), D-mannose (>99%, Sigma-Aldrich), 1,6-anhydro- β -D-glucose (levoglucosan, >99%, Sigma-Aldrich), 5-

hydroxymethyl furfural (HMF, 98% AK Scientific), acetone (HPLC grade, Fisher Scientific), DOWEX monosphere 99 Ca/320 separation resin (DOW), Amberlyst-15 (hydrogen form, Sigma-Aldrich), Glucose isomerase (≥ 350 unit·g⁻¹, from *Streptomyces murinus*, Sigma-Aldrich), quartz wool (Ohio Valley Specialty), Silicon dioxide (99.9%, 4-20 mesh, Sigma-Aldrich), Milli-Q water (~ 18 M Ω cm), 10 ml glass reactor (Chemglass), and straight bore burette with PTFE stopcock (100 mL, Kimble Kimax, Class A).

Product analysis (HPLC)

The concentrations of the components of the isomerized and dehydrated solution were quantified by High Performance Liquid Chromatography (HPLC) analysis using a Bio-Rad Aminex HPX-87H column on a Waters 2695 system equipped with RI-2414 and PDA-2998 detectors in series. Glucose, fructose, HMF, sugar by-products (cellobiose, levoglucosan, mannose), and levulinic acid were calibrated using standard solutions. An aliquot of the product mixture was diluted 10 times with Milli-Q water and was filtered through a 0.2 μ m PTFE filter before analysis. The temperature of the HPLC column was maintained at 50°C, and the flow rate of the mobile phase (pH 2 water, acidified by sulfuric acid) was kept constant at 0.6 mL·min⁻¹. Glucose, fructose, sugar by-products, and levulinic acid were analyzed by a RI detector, while the HMF concentration was measured with a Waters 2998 PDA detector at 320 nm. The conversions and yields were calculated by the following equations.

$$\text{HMF yield from fructose} = \frac{\text{Moles of final HMF}}{\text{Moles of initial fructose}} \cdot 100 (\%)$$

$$\text{Fructose conversion} = \frac{\text{Moles of initial fructose} - \text{Moles of final fructose}}{\text{Moles of initial fructose}} \cdot 100 (\%)$$

$$\text{Glucose conversion} = \frac{\text{Moles of initial glucose} - \text{Moles of final glucose}}{\text{Moles of initial glucose}} \cdot 100 (\%)$$

Enzymatic isomerization of glucose in acetone/water (80/20, v/v) solvent

0.38 g of glucose was dissolved in 1.6 mL of Milli-Q water to prepare an aqueous glucose solution (19wt% glucose). 5 g of acetone was added to the aqueous glucose solution for preparing acetone/water (80/20, v/v) solvent. 0.25 g of immobilized glucose isomerase (from *Streptomyces murinus*) was ground and added to the glucose feed. The glass vial reactor was placed in an oil bath at 65°C and the feed solution was stirred at 560 rpm. Reaction time was varied from 10 to 180 min. After the reaction, the product solution was quenched in water bath to stop the reaction. 21 mol% of sugars were precipitated with the enzyme as the temperature decreased from 65 to 20°C. The quenched solution was centrifuged at 3000 rpm for 10 min to separate the precipitate from the liquid solution. 0.5 mL of separated liquid solution was diluted 10 times with Milli-Q water and filtered through a 0.2 μ m PTFE filter before analysis. 8 mL Milli-Q water was added to the precipitated (mixture of glucose, fructose, enzyme) to dissolve the sugars in aqueous solution. The aqueous sugar solution was analyzed without dilution.

Dehydration of simulated isomerization solution over Amberlyst-15

A simulated isomerization solution was prepared as the feed for dehydration reaction. 0.14 g of glucose and 0.23 g of fructose were

dissolved in 1.6 mL of Milli-Q water. 5.0 g of acetone was added into the aqueous sugar solution. 0.2 g of Amberlyst-15 (40 μ m to 150 μ m) was mixed with the feed in 10 mL thick-walled glass reactors (Chemglass) and placed in an oil bath at 120 °C. A triangular stir bar was used to stir the reaction mixture at 750 rpm. Reaction time was varied from 40 to 100 min. After dehydration, the product solution was quenched in a water. The quenched solution was centrifuged at 3000 rpm for 10 min to separate the solid catalyst. 0.5 mL of the dehydrated solution was diluted 10 times with Milli-Q water and filtered through a 0.2 μ m PTFE filter for HPLC analysis.

Column chromatography separation of glucose, fructose, and HMF

0.69 g of glucose, 0.09 g of fructose, and 0.70 g of HMF were dissolved in a mixture of Milli-Q water (9.57 g) and acetone (30.11 g) to prepare the simulated solution in Figure 2. 100 mL (apparent volume) of dry resin (DOWEX 99 Ca/320) was stirred in 400 mL of acetone/water (80/20, v/v) solvent for 15 min and the resin was filtered. These washing cycles were repeated 5 times to prepare the wet resin for chromatographic separation. The chromatography column was prepared by filling a 100 mL straight bore buret with quartz wool, silicon dioxide, and 42 mL (apparent volume) of wet resin (void fraction = 0.3). The desorbent flow was driven by gravity, resulting in monotonic decrease of the desorbent velocity, because the level of desorbent in column decreased with time proceeding the separation. The linear velocity profiles of the loaded feed and the desorbent during the separation are shown in Figure S3. Slow flow rate of the loaded feed facilitated HMF separation from sugars by maximizing the contact time of the chemicals and the resin, whereas a faster flow of the desorbent was used to recollect glucose and fructose after HMF collection. 42 mL of the simulated solution was loaded on the column. Then, the desorbent (acetone/water (80/20, v/v) solvent) was slowly added (Figure S3 (a)) to initiate chromatography of the loaded sample to separate HMF. After 85 mL of eluent collection for HMF isolation, 2.5 L of desorbent was passed through the column with fast low rate (Figure S3 (b)) to recollect glucose and fructose. The eluent samples from the chromatography were injected into the HPLC after filtration by 0.2 μ m PTFE filter without dilution for analysis.

Adsorption isotherms of glucose, fructose, and HMF on resin

The wet resin was dried by vacuum treatment on filter paper. Different amounts of glucose (0.02, 0.04, 0.06, 0.08, 0.1 g) were dissolved in 5 mL of acetone/water (80/20, v/v) solvent, and 0.1 g of dried resin was added to each glucose sample. Then, the set of five glucose solutions, containing the dried resin, was placed in an oil bath at different temperatures (23, 40, 55°C). Five fructose samples (0.02, 0.04, 0.06, 0.08, 0.1 g of fructose with 0.1 g of dried resin in 5 mL of acetone/water solvent) were prepared for fructose adsorption experiments. Then, the set of five fructose samples was placed in an oil bath at different temperatures (24, 40, 60°C). A set of HMF adsorption experiments was prepared by mixing 0.02, 0.04, 0.06, 0.08, 0.1 g of HMF with 0.1 g of dried resin in 5 mL of acetone/water solvent. Then, the set of HMF samples with resin was placed in an oil bath at different temperatures (24°C). All the samples were stirred at 750 rpm for overnight (13-15 h). 0.2 mL of samples from HMF, glucose and fructose adsorption experiments were diluted 3 times in Milli-Q water and filtered by 0.2 μ m PTFE

filter for HPLC analysis. The adsorbed amounts of chemicals were calculated by comparing the chemical concentrations before and after the adsorption. The adsorption equilibrium constants and

$$\text{Langmuir isotherm adsorption: } q = q_{\max} \frac{K_{ads}C}{1+K_{ads}C}$$

$$\text{Linear isotherm adsorption: } q = K_{ads}C$$

Where, q : adsorbed amount of chemical (g chemical /g resin), q_{\max} : maximum adsorbed amount of chemical (g chemical /g resin), C : chemical concentration in solution (mol/L), K_{ads} : adsorption constant (L/mol).

$$\text{Adsorbed chemical amount} = \frac{\text{Mass of dissolved chemical before adsorption} - \text{Mass of dissolved chemical after adsorption}}{\text{Mass of resin}} \text{ (g/g)}$$

Results and Discussion

Enzymatic glucose isomerization and acid-catalyzed fructose dehydration

Immobilized glucose isomerases have been used for industrial scale processes of HFCS production due to their high activity and stability²⁷. Over 500 tons of the immobilized enzymes are synthesized and enable the production of approximately 10 million tons of HFCS per year²⁸. We used the commercial immobilized enzyme ($\geq 350 \text{ unit}\cdot\text{g}^{-1}$) from *Streptomyces murinus*, to catalyze glucose isomerization to produce fructose in an acetone/water (80/20, v/v) solvent at 65°C. Note that the use of acetone solvent enhanced the activity and stability of the enzyme for isomerization²⁹. The concentration (5.4 wt%) of glucose in an acetone/water (80/20, v/v) solvent was the upper solubility limit at the reaction temperature (65°C). As shown in Figure S1, a 5.7 wt% glucose solution was not soluble in acetone/water at 65°C, whereas 5.4 wt% glucose solution was soluble. Fructose has higher solubility (Figure S1(c)) than glucose in an acetone/water solvent and shows mono-phasic product solution at 65°C after isomerization. Thermodynamic equilibrium was obtained after 40 min of reaction, resulting in 61.3% glucose conversion and >98% fructose selectivity in Figure 1(a). Enzymatic isomerization reaches thermodynamic equilibrium ($K_{eq}=1.59$) after 40 min of reaction at 65°C, compared to Sn- β catalyst (with the reaction quotient, $Q=0.75$, from previous work) at 80°C after 180 min of reaction¹⁸. Fructose dehydration in an acetone/water (80/20, v/v) solvent was investigated over Amberlyst-15 catalyst at 120°C. The highest HMF yield (78.7%) and 91.3% conversion of fructose was obtained at 90 min as shown in Figure 1(b). A reaction time of 100 min resulted in decreased HMF yield due to the production of levulinic acid by the acid-catalyzed rehydration of HMF³⁰. The HMF selectivity varied between 80-86% during fructose dehydration.

adsorbed amounts (measured by HPLC) were calculated by the following equations.

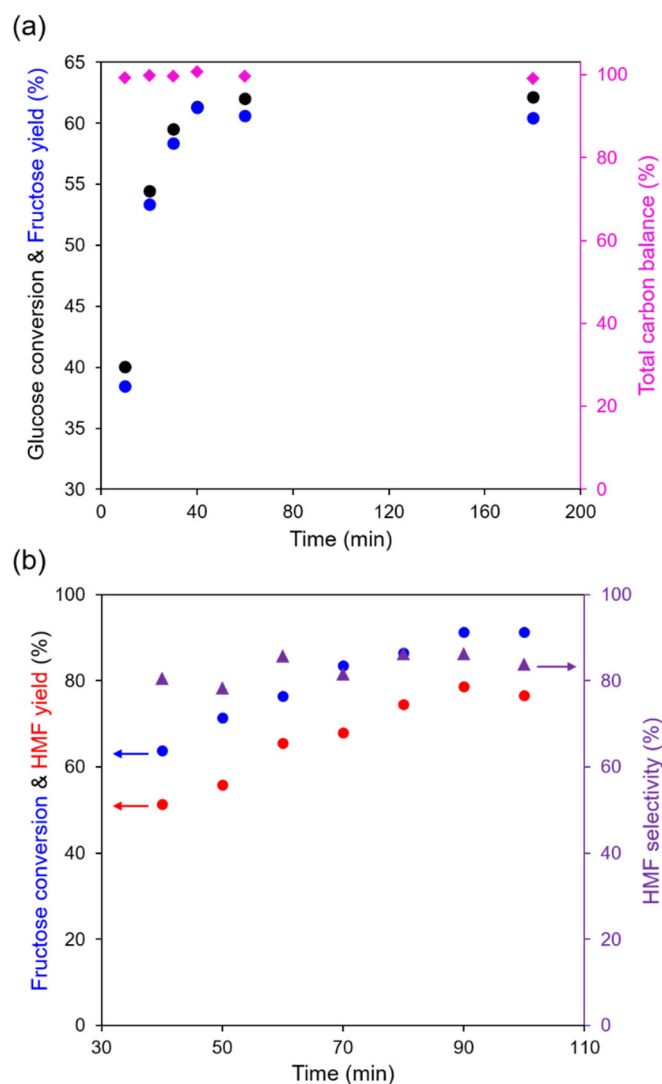


Figure 1. (a) Enzymatic isomerization of glucose (5.4wt%, 270 mM) in acetone/water (80/20, v/v) solvent at 65°C (black dot: glucose conversion, blue dot: fructose yield, pink diamond: total carbon balance); (b) Acid-catalyzed fructose (7.4wt%, 388 mM) dehydration over Amberlyst-15 catalyst in acetone/water (80/20, v/v) solvent at 120°C (blue dot: fructose conversion, red dot: HMF yield, purple triangle: HMF selectivity).

In subsequent experiments, HMF was produced from glucose (5.4 wt%, 270 mM) by sequential reactions of enzymatic isomerization followed by acid-catalyzed fructose dehydration as shown in Figure 2(a). Glucose was converted to fructose in an acetone/water (80/20, v/v) solvent by isomerization without significant by-product

(mannose, cellobiose, anhydro-sugar) formation (<2% selectivity). A simulated solution (glucose and fructose mixture in an acetone/water solvent) was used to investigate the dehydration since 25 mol% of glucose and 18 mol% of fructose were precipitated with the enzyme during the temperature quenching (from 65 to 20°C) after isomerization. Figure 2(b) shows the overall moles of consumed sugars and the produced chemicals by the dehydration over Amberlyst-15. 88.9% fructose and 14.1% glucose were converted to HMF and by-products, including sugar by-products, levulinic acid, and humins. The selectivity of HMF, sugar by-products, and levulinic acid were 78.6%, 15.2%, and 3.2%, respectively. 3.0% of glucose and fructose were converted to water-soluble humins by acid-catalyzed self-condensation. The humins can be selectively adsorbed on activated carbon and purged by filtering the activated carbon¹⁸. The three major chemicals in the dehydrated solution are HMF, glucose, and fructose (Figure S2).

the dehydration reaction in 8 mL dehydrated solution. (Reaction conditions: glucose isomerization was operated at 65°C for 40 min over enzyme; fructose dehydration operated at 120°C for 90 min over Amberlyst-15; Acetone/water (80/20, v/v) solvent was used in both the reactions.)

Chromatographic separation of glucose, fructose, and HMF

A simulated solution, containing the major three compounds (glucose, fructose, HMF) in the dehydrated solution (Figure S2), was prepared to demonstrate the chromatographic separation at room temperature (23–25°C). The three compounds (89% mole fraction) were quantified by HPLC analysis, while each by-product was not detected by HPLC because of its low concentration (2–4%) after dilution by the chromatographic desorbent. The concentration of the major chemicals (80 mM glucose, 10.5 mM fructose, 116 mM HMF) in the simulated solution was the same as the experimentally obtained products (Figure 2(a)). The acetone/water (80/20, v/v) solvent was used as the desorbent during chromatography, and DOWEX 99 Ca/320 as the chromatography resin. HMF was firstly eluted by the chromatographic separation (Figure 3(a)). Therefore, the initially collected sample contained pure HMF (>99% purity by HPLC) in the acetone/water desorbent. Then, glucose and fructose followed the HMF collection. Glucose had a smaller retention volume than fructose (inset of Figure 3(a)). All the loaded HMF was collected at desorbent/feed (v/v) ratio = 0.6 (Figure 3(b)). Similarly, 100% of loaded glucose and 61% of loaded fructose were collected at desorbent/feed (v/v) = 22 (Figure 3(c)). The fructose required large volume of desorbent to be removed from the resin. For example, when 92% of loaded fructose was recovered, 58 times higher volume of desorbent was required than the volume of the loaded feed (desorbent/feed (v/v) = 58) (Figure 3(d)).

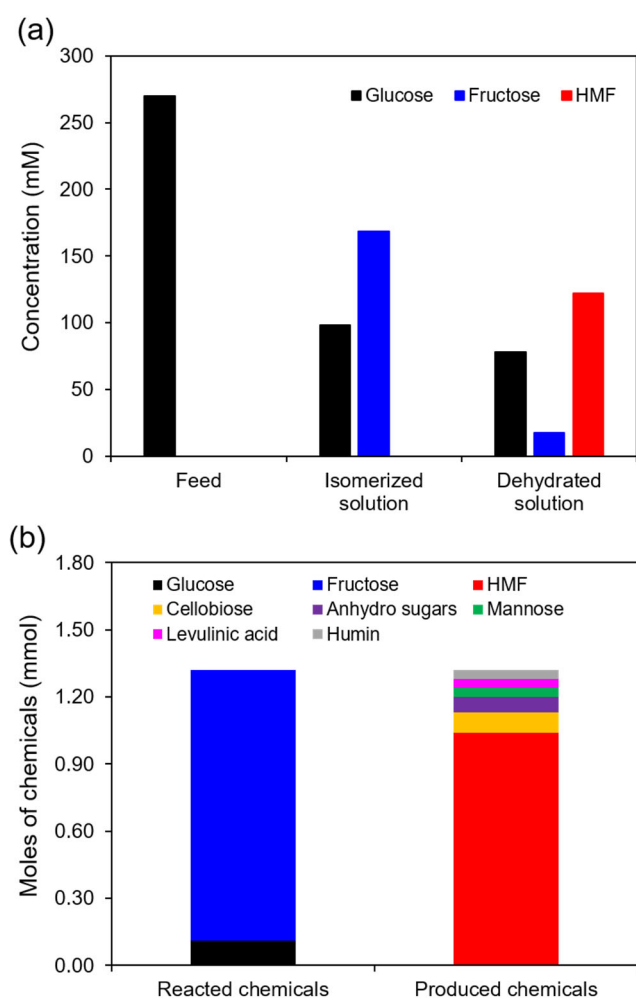


Figure 2. (a) Concentrations of glucose, fructose and HMF in the reacted solution; (b) Moles of reacted and produced chemicals by

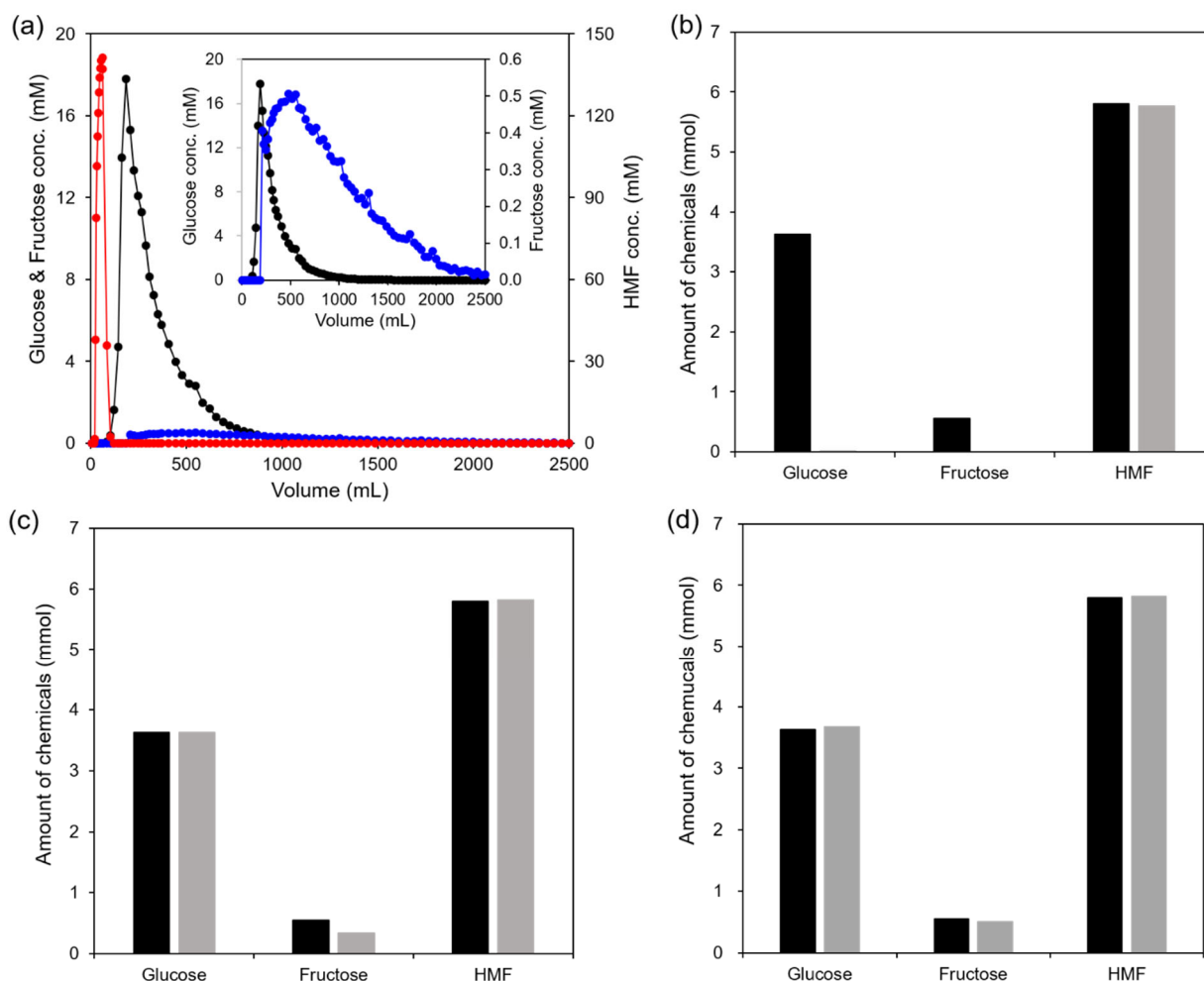


Figure 3. (a) Concentration profiles of glucose (black), fructose (blue), and HMF (red) during the experimental chromatography separation at room temperature (23–25°C). Acetone/water (80/20) solvent was used as desorbent to separate HMF, glucose and fructose. Inset figure represents magnified concentration profiles of glucose and fructose (solid lines are the visual guidance); Comparison of chemical amounts 'before (black bar)' and 'after (grey bar)' the chromatography at different desorbent/feed (v/v) ratios, (b) desorbent/feed (v/v) = 0.6, (c) desorbent/feed (v/v) = 22, (d) desorbent/feed (v/v) = 58. (Loaded feed conditions: 80 mM glucose, 10.5 mM fructose, 116 mM HMF in acetone/water (80/20, v/v) solvent).

Adsorption model for glucose, fructose, and HMF on the chromatography resin

Equilibrium adsorption isotherms for glucose, fructose, and HMF on the chromatography resin (DOWEX 99 Ca/320) were obtained at 23–24°C (Figure 4). Fructose was the most strongly adsorbed component and followed a Langmuir adsorption isotherm at 24°C. The adsorption equilibrium constant and the maximum adsorbed amount of fructose were estimated to be $7.13 \pm 2.09 \text{ L} \cdot \text{mol}^{-1}$ and $0.44 \pm 0.08 \text{ g fructose} \cdot \text{g resin}^{-1}$ (95% confidence interval), respectively. Glucose was weakly adsorbed and followed a linear isotherm adsorption model at 23°C with $1.28 \text{ L} \cdot \text{mol}^{-1}$ of adsorption equilibrium constant. HMF showed no adsorption at 24°C. The adsorption models for glucose, fructose, and HMF explain the separation order of the loaded chemicals in the chromatography separation. Specifically, adsorption of fructose on resin contributes to the longest elution time, whereas HMF passes through the column fastest since it is not adsorbed on the resin.

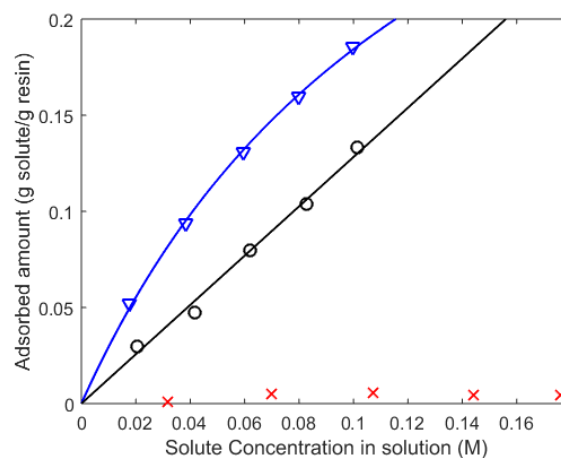


Figure 4. Isothermal adsorption of fructose (blue triangle), glucose (black circle), and HMF (red cross) on DOWEX 99 Ca/320 at 23–24°C. Adsorption model: Langmuir isotherm adsorption (blue line), linear

isotherm adsorption (black line); Adsorption temperature was at 23-24°C.

Adsorption thermodynamic parameters of glucose and fructose

The adsorption equilibrium constants of fructose and glucose were measured at different temperatures to determine the adsorption thermodynamic parameters (ΔH_{ads} , ΔS_{ads}). The adsorption equilibrium constant of fructose was calculated to be 7.13, 5.40, and 4.49 $\text{L}\cdot\text{mol}^{-1}$ at 24, 40, and 60°C, respectively. The maximum adsorption capacity of fructose was determined to be 0.42 g fructose/g resin based on the Langmuir isotherm adsorption model in Figure 5(a). The glucose adsorption constant was 1.28, 1.22, and 1.17 $\text{L}\cdot\text{mol}^{-1}$ at 23, 40, and 55°C, respectively (Figure 5(b)). The adsorption enthalpy (ΔH_{ads}) and entropy (ΔS_{ads}) of the fructose and glucose on the resin were calculated by Figure 5(c) and (d). ΔH_{ads}

and ΔS_{ads} for fructose adsorption were estimated to be $-10582 \pm 910 \text{ J}\cdot\text{mol}^{-1}$, and $-19.3 \pm 2.9 \text{ J}\cdot\text{mol}^{-1}\text{K}^{-1}$, respectively (90% confidence interval). For glucose adsorption, ΔH_{ads} and ΔS_{ads} were $-2321 \pm 198 \text{ J}\cdot\text{mol}^{-1}$, and $-5.8 \pm 0.6 \text{ J}\cdot\text{mol}^{-1}\text{K}^{-1}$ (90% confidence interval), respectively. The adsorption thermodynamic parameters were used to optimize the simulated-moving-bed (SMB) separation in techno-economic analysis model. The retention times of the by-products (e.g., cellobiose, mannose, anhydro-sugar, levulinic acid) are similar (7-17 min) to glucose and fructose (9-10 min) in high-performance liquid chromatography (HPLC) analysis (Figure S4), whereas retention time of HMF is relatively high (retention time: 34 min). This result indicates that the by-products can be collected along with fructose by chromatographic separation. Thus, the adsorption thermodynamic parameter of fructose was used to simulate the separation of by-products for the SMB model in TEA.

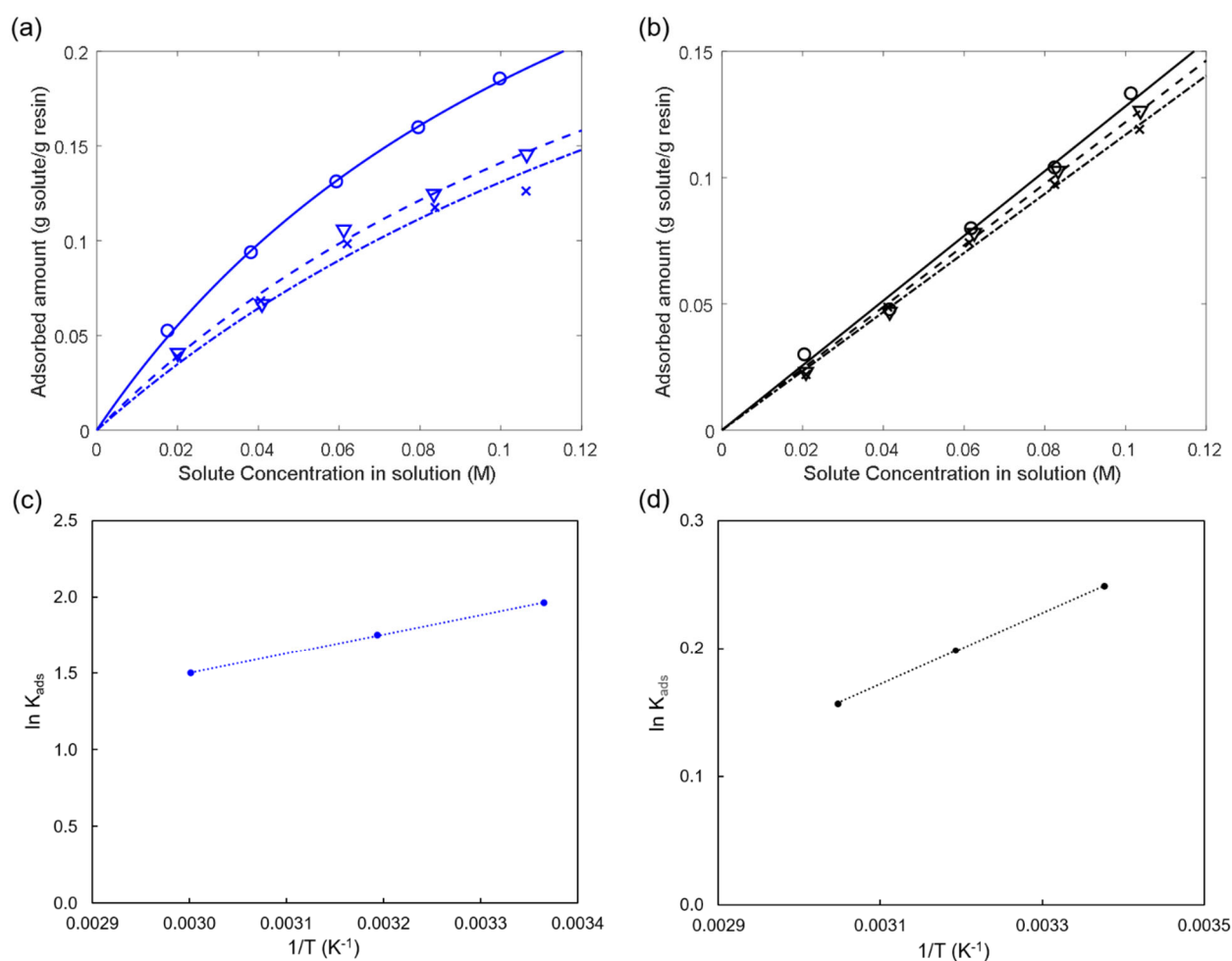


Figure 5. Adsorption isotherms of glucose and fructose at different temperatures (a) Langmuir isotherm adsorption of fructose at different temperatures (circle: 24°C, triangle: 40°C, cross: 60°C), (b) linear isotherm adsorption of glucose at different temperatures (circle: 23°C, triangle: 40°C, cross: 55°C); Van't Hoff plot of (c) fructose adsorption and (d) glucose adsorption.

System-level studies of HMF production process

We developed a process model for production of HMF from glucose (shown in Figure 6(a)), using the experimental data in this paper and Aspen Plus Process Simulator (V10.0 Aspen Technology). A complete material balance is shown in Table S1. These data were then used to perform a techno-economic analysis. Experimental

results were used to model the reactors and adsorption column for separating humins, whereas Aspen was used to model the evaporators. The glucose feed is combined with an acetone/water stream and a glucose, fructose, H_2O , and acetone recycle stream and fed into the isomerization reactor (R-1). The products from R-1 are then dehydrated in R-2. The products are then passed over an activated carbon bed that removes the humins. It is assumed

that 1% of sugars and by-products are also lost with humins. The products are then sent to a simulated moving bed (SMB) separator (S-2). S-2 separates the HMF from the glucose and fructose. We modeled a SMB for separation which is more industrially practical than batch chromatography as used in our experiments. The batch chromatography uses a higher volume of desorbent than SMB and is not a continuous process³¹. SMB was modeled and simulated in Aspen Chromatography (V10.0 Aspen Technology) using the isotherm parameters obtained in Figure 4. A molecular sieve column (S-4) was used to remove excess water formed in the dehydration reactor. We optimized the design and operating conditions of SMB, and obtained HMF recovery and purity of 96.5% and 96.8%, respectively in the raffinate stream using a desorbent/feed ratio (v/v) of 1.12 (Figure S5).

100% of glucose and 85.3% of fructose are recovered in the extract stream (stream 9), whereas 96.5% of HMF is recovered in the raffinate stream (stream 8). It is assumed that the sugar by-products and levulinic acid are recovered in the extract stream. The volumetric flow rate of the raffinate is 0.97 times the SMB feed (stream 6). Stream 8 is then passed through a series of flash columns operating at low temperatures and pressures to separate

HMF from the solvent. Stream 10 containing acetone/water solvent is passed through a molecular sieve adsorber to remove excess water formed in the dehydration reactor. It is assumed that 1% of acetone is also lost with water.

Based on the optimization results of SMB, the volumetric flow rate of desorbent (stream 14) needs to be 1.12 times the volumetric flow rate of feed (stream 6). A part of the desorbent requirement is fulfilled by stream 12 and the rest is satisfied by separating the solvent from the extract. First, stream 9 is split in two streams. One of them (stream 15) is passed through a flash column operating at 90°C to separate sugars from the solvent system. The solvent stream (stream 17) is combined with stream 12 to satisfy the requirement on desorbent amount. To prevent accumulation of by-products, a fraction of stream 18 is discharged and sent to the waste treatment facility. The remaining fraction (stream 19) is combined with stream 16 and recycled to the isomerization reactor. A base design case is simulated by considering the glucose feed flow rate of 2000 kg·h⁻¹ resulting in annual HMF production of 8.74 kton. The material balance information for the main streams is given in Table S1.

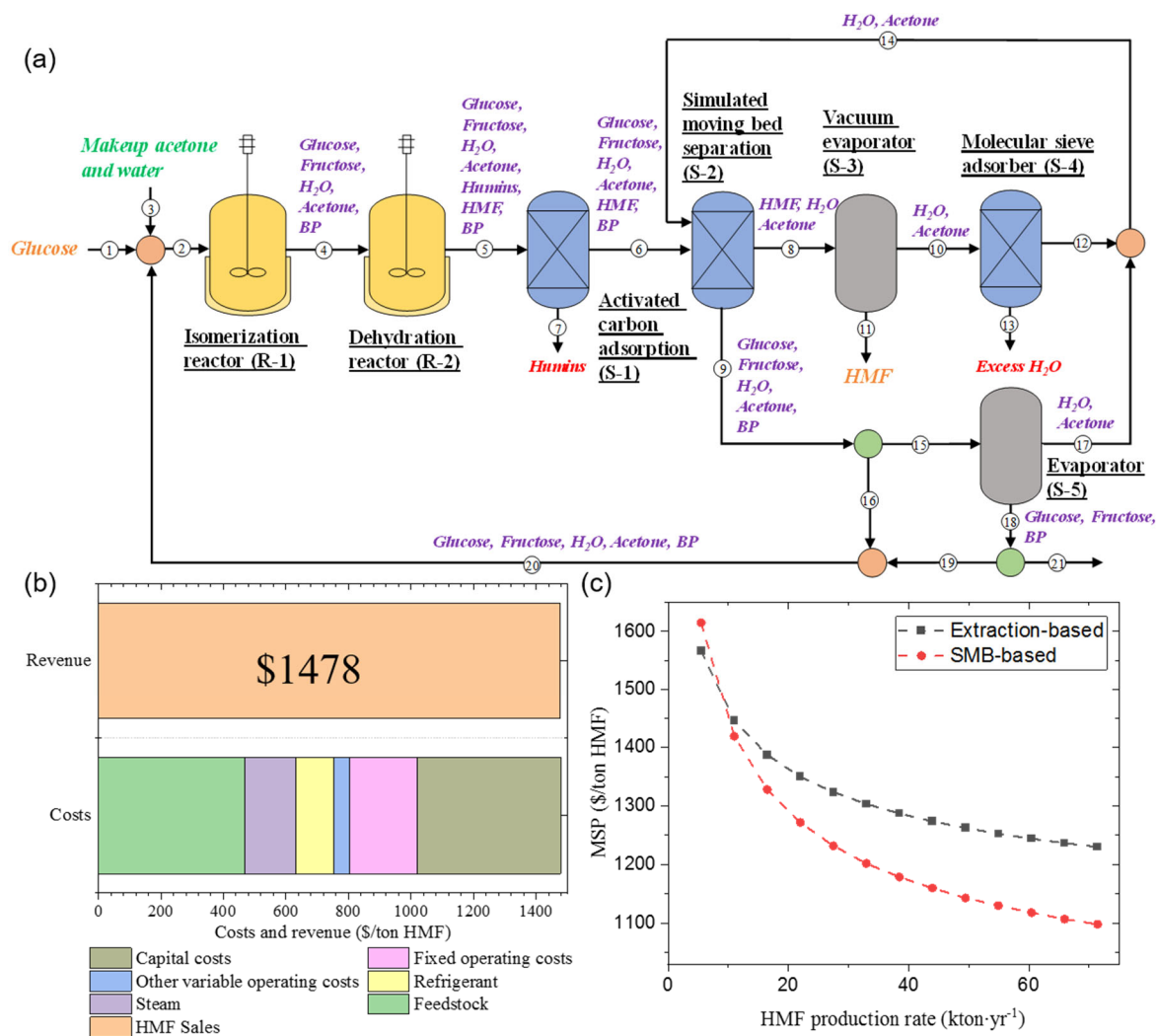


Figure 6. (a) Overall process flow diagram for production of HMF; (b) A summary of costs and revenue of the proposed process; (c) Comparison of MSP of extraction and SMB-based approaches with feedstock flowrate.

Next, we estimated the total energy requirements of the process. It is assumed that steam, cold water, refrigerant, and electricity are available for purchase to meet the heating, cooling, and power requirements, which are 15.4 MW, 19.3 MW, and 24.2 kW, respectively. 24% of the cooling requirements are satisfied by the refrigerant and the remaining by cooling water.

After modeling the process in Aspen Plus, capital and operating costs of the process were estimated. To provide a fair comparison with another HMF production process¹⁸, the equipment and material costs are adjusted to a common basis year of 2017. The unit installed cost, C , for capacity S in the cost-year is computed using,

$$C = C_0 \left(\frac{S}{S_0} \right)^\beta \left(\frac{I_{cost}}{I_{base}} \right) \quad (1)$$

where C_0 is the installed cost for capacity S_0 in the base year, and I_{cost} and I_{base} are the plant cost indices in the cost and base years, respectively. The parameters in Eq. (1) of the main equipment are given in Table S2. Once the total equipment cost has been determined, the total capital investment (TCI) is estimated by considering other direct and indirect costs (summary in Table S3). For the base design of the HMF plant producing 8.74 kton/yr, TCI is estimated to be \$31.8 million.

The operating costs of the process comprise of fixed and variable components. The fixed operating costs consist of labor and other overhead items. The variable operating costs are estimated based

on the utility, catalyst, and raw material (feedstock and makeup chemicals) consumption. The total operating costs are estimated to be \$8.9 million/year (summary in Table S4).

Based on the estimated capital and operating costs, and the economic parameters listed in Table S5, the minimum selling price (MSP) of HMF was computed using discounted cash flow analysis. The MSP of HMF was calculated to be \$1478/ton (Figure 6 (b)) for the base design.

We also compared the economics of the proposed approach with an extraction-based process, where methyl isobutyl ketone (MIBK) was used as a solvent to extract HMF from sugars¹⁸. After extraction, HMF was separated from MIBK by vacuum evaporation. Thus, vacuum evaporation was required to separate (i) MIBK from HMF and (ii) HMF from the solvent system. The SMB approach does not require MIBK. In the SMB approach, vacuum evaporation is required only once to separate HMF from the solvent. A summary of the differences between the two approaches is given in Table 1. The extraction-based approach has a lower capital, higher yield, and higher variable operating costs than the SMB approach. The higher capital cost for the SMB approach is because of high SMB cost. The higher yield of the extraction-based approach is because of higher selectivity in dehydration reaction. The MSP of the extraction-based approach is slightly less than the proposed SMB-based approach for the base case.

Table 1. Economic analysis of producing 8.74 kton HMF annually using Extraction-based and SMB-based approaches.

Process	Glucose concentration (mM)	Yield (g HMF/g glucose)	Capital costs (\$/ton)	Variable operating costs (\$/ton)	Fixed operating costs (\$/ton)	MSP (\$/ton)
Extraction-based	222	0.63	357	961	165	1483
SMB-based	270	0.5	459	804	215	1478

The equipment costs and fixed operating costs exhibit economies of scale. However, the variable operating costs, which account for a significant share of the total operating costs for the two processes, vary linearly with scale. A comparison of the variable operating costs of the two approaches is shown in Figure S6. The SMB approach leads to 16% reduction in the variable operating costs compared to the extraction-based approach mainly due to the elimination of MIBK use and reduced refrigerant consumption. Thus, the proposed approach becomes more competitive with increase in the process scale as illustrated in Figure 6(c). The analysis suggests that for a facility producing more than 8.39 kton-yr⁻¹ of HMF, it is more economical to use the SMB-based approach.

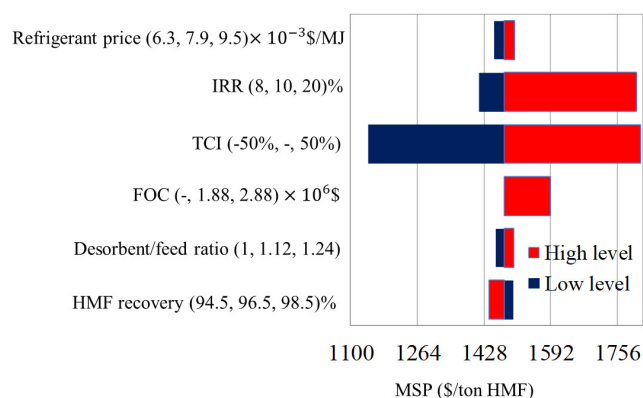


Figure 7. Sensitivity analysis results.

We performed sensitivity analyses with respect to technical (e.g. HMF recovery using SMB and desorbent/feed ratio for SMB) and economic parameters (e.g. refrigerant prices, ROI discount rate, total capital investment, and fixed operating costs) to identify the major cost drivers. Each variable was changed to a minimum and maximum value with all other variables held constant. The results are shown in Figure 7. Although refrigerant satisfies only 24% of the cooling requirements, it contributes moderately (8%) to the MSP

because of its high price. A 20% reduction in the refrigerant price leads to 1.6% reduction in the MSP. Internal rate of return (IRR) also greatly impacts the MSP. If the IRR is increased to 20%, the MSP of HMF increases to \$1800. In general, capital costs are subject to significant uncertainty, especially when pioneer plants are constructed.³² A $\pm 50\%$ variation in total capital investment changes the MSP by 22.7%. For the sake of simplicity, fixed operating costs (FOC) are computed based on the capital investment for the base design case. However, for a small-scale plant, this method most likely underestimates the labor costs component of FOC. We estimate the labor costs based on the number of operators and see that the FOC increases by \$1 million, resulting in an increase in MSP by 7.6%.

We study the impact of SMB performance on MSP of HMF. The results obtained in the current study are based on conventional SMB comprising of four sections with five columns in each section. The development of alternative operation modes (e.g., dynamic configuration variations and flow rate modulations)³³ and optimization of column configurations have shown to enhance product purity, recovery, and productivity, and reduce the required number of columns. We study two parameters related to SMB performance – desorbent/feed ratio and HMF recovery. While increasing the former increases the capital costs and energy consumption of the evaporator S-5 and increases the MSP, increasing the latter improves the overall HMF yield and reduces the MSP.

Integration with HFCS production facility

High fructose corn syrup (HFCS) is a sweetener made from milled corn and used predominantly in food and beverage industries. It became popular in the late 1970s when the price of regular sugar was high. However, due to the ongoing debate regarding its correlation to obesity and heart disease, the industry has

experienced decreased demand over the past several years. We now show that by integrating HMF production process in a corn biorefinery producing HFCS, the economics of the biorefinery can be improved.

An integrated process for the production of HFCS and HMF is shown in Figure 8. First, corn is wet milled to recover and purify starch and other coproducts. The first step in wet milling involves softening the texture of corn kernel by soaking it in water and sulfur dioxide. The grain is then ground and the constituents are separated by screening, washing, hydrocloning, and centrifuging. More details on the wet milling process can be found in Blanchard³⁴. The end products of wet milling are germ, corn gluten feed, corn gluten meal, and starch. The germ is used to produce corn oil, which has applications in food and cosmetic industries. Corn gluten feed is high fiber, low protein feed for beef cattle. Corn gluten meal contains high protein and low fiber, used to feed poultry and swine. While starch can be used as a food additive or adhesive with minimal further processing, its conversion to sweeteners is economically more favorable. Thus, starch is hydrolyzed to yield a syrup with over 95% glucose (dry solids basis) and the remaining sugars are maltose, maltotriose with traces of higher oligomerized sugars. A fraction of the glucose stream is sent to the syrup production section, where glucose is converted to fructose such that concentration of fructose is 42% on a dry weight basis. The converted HFCS-42 syrup is further purified and concentrated. Generally, the remaining glucose stream is sold as a coproduct, but we propose to use it to produce HMF. We perform technoeconomic analyses for the integrated HFCS/HMF process considering two systems for different fractions of glucose going to either produce HMF or HFCS. First, we analyze the economics of building a new facility for the integrated process. Second, we examine retrofitting an existing HFCS production facility to produce HMF.

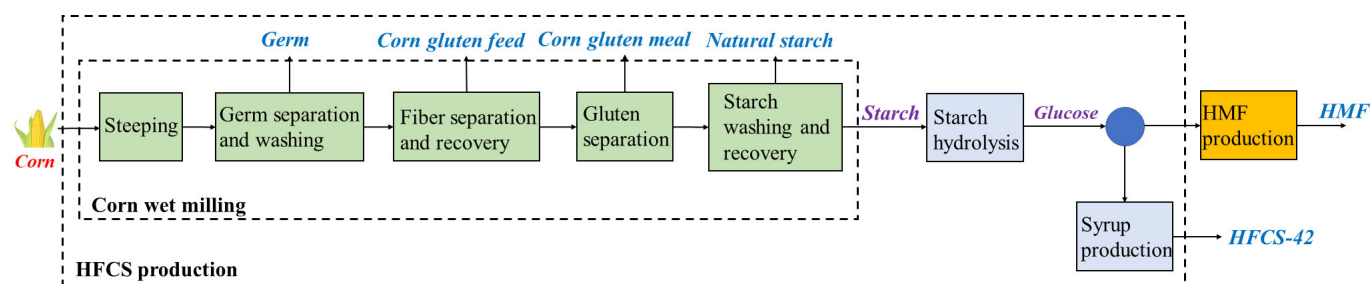


Figure 8. An overview of integrated HFCS/HMF process.

We use SuperPro Designer model by Intelligen³⁵ to perform mass and energy balances, and estimate capital and operating costs of the HFCS process. A base design is considered with a corn feed flow rate of 50000 kg·h⁻¹. TCI and operating costs are estimated to be \$189.4 million and \$123.7 million/year, respectively for the greenfield facility. The relevant parameters for the analysis are given in Table S6.

We analyze the process and economic conditions that make the integrated HFCS/HMF process economically more favorable than the HFCS process. The results of the analyses are shown in Figure 9. One of the glucose streams from the starch hydrolysis section is used to produce HFCS-42, whereas the other stream is either sold as a by-product in HFCS process or utilized to produce HMF in

HFCS/HMF process. The combined HFCS/HMF process requires more capital investment than the HFCS process alone. The amount of HMF produced is less compared to glucose produced by HFCS process. Therefore, the selling price of HMF needs to be higher for the integrated HFCS/HMF process to be more economically favorable. For the analysis shown in Figure 9 (a), we have assumed HMF price to be \$1500/ton. To understand the effect of changing the production rate of HFCS-42 on the economics of the two processes, we estimate the MSP of HFCS-42 and IRR. MSP is estimated based on 15% IRR. The results are shown in Figure 9 (a). While the MSP of HFCS-42 increases with decrease in its production rate for the two processes, we see that MSP is lower for HFCS/HMF process if the production rate of HFCS-42 is lower than 185 kton/yr

(fraction of glucose sent to syrup production, $f_{g \rightarrow \text{HFCS}} = 0.93$). Thus, a corn refinery using integrated HFCS/HMF process can afford to offer HFCS at a lower price and be more competitive. We also observe that IRR decreases with decrease in production rate, however, it decreases more rapidly for HFCS process. The analysis suggests that in comparison to glucose, HMF compensates for the loss in revenue due to lower HFCS production to a higher degree and therefore, it is more economical to convert the glucose stream to produce HMF.

Clearly, for HFCS/HMF process to be more profitable, the selling price of HMF needs to be higher than glucose and it needs to be produced at sufficiently large scale to take advantages of economies of scale. Figure 9 (b) shows that with increase in the price difference between HMF and glucose, and decrease in HFCS-42 production, HFCS/HMF process becomes more favorable.

function of fraction of glucose sent to syrup production section ($f_{g \rightarrow \text{HFCS}}$) for HFCS and HFCS/HMF processes. (b) Difference in the net present values (NPV) of HFCS/HMF and HFCS processes as a function of difference in glucose and HMF selling price and $f_{g \rightarrow \text{HFCS}}$.

Now, we consider the brownfield system wherein an existing HFCS facility that is fully depreciated is retrofitted to integrate an HMF production section. Compared to a stand-alone HMF production system, this system is expected to reduce costs and investment risks because of existing energy recovery facilities, experienced workforce and a reliable source of feedstock. In a study by de Jong et al.³⁶, the benefits of retrofitting were quantified and the authors estimated a 12% reduction in total capital investment compared to a stand-alone plant because of reduced capital expenditures for buildings, service facilities, land and yard works. A comparison of TCI for a stand-alone HMF, greenfield and brownfield HFCS/HMF systems for different production capacities of HMF is given in Table 2. TCI for a brownfield system is an order of magnitude lower than a greenfield system and 12% lower than a stand-alone HMF system. Moreover, with declining market of HFCS, it is less risky to retrofit an existing HFCS plant than constructing a new HFCS/HMF facility.

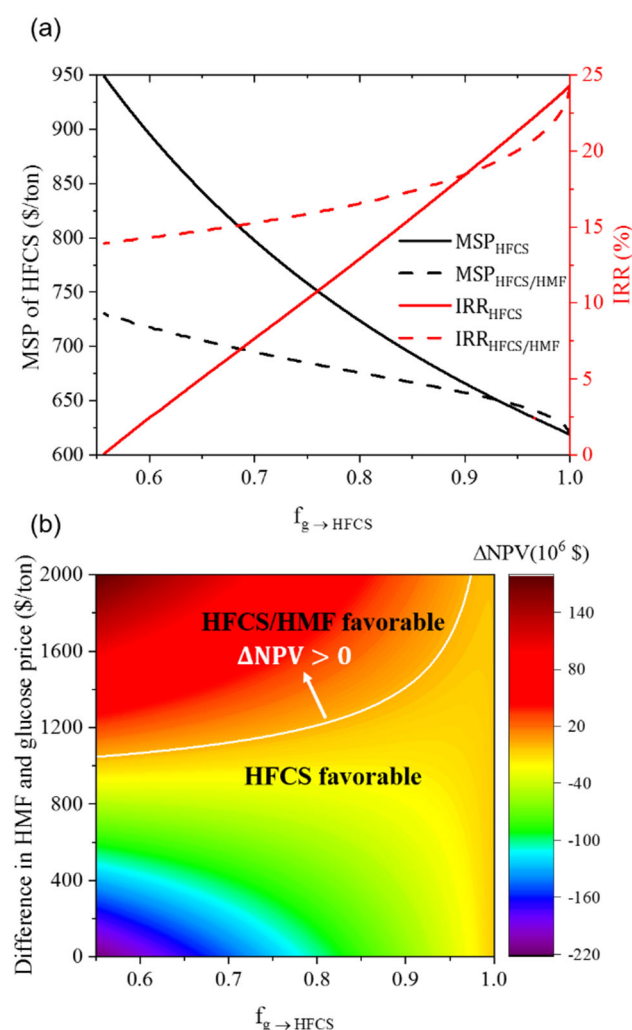


Figure 9. Economic analyses and comparison of greenfield HFCS/HMF and HFCS systems. (a) MSP of HFCS-42 and IRR as a

Table 2. TCI for a stand-alone HMF system, greenfield and brownfield HFCS/HMF systems.

HMF production (kton/yr)	TCI for stand-alone HMF system (MM\$)	TCI for greenfield HFCS/HMF system (MM\$)	TCI for brownfield HFCS/HMF system (MM\$)
3.5	18.4	208.4	16.2
9.2	32.8	222.5	28.9
17.5	48.3	237.4	42.5

To determine whether retrofitting an existing HFCS plant to integrate an HMF production section is advantageous, we use marginal payback period (MPBP) and marginal return on investment (MROI) as the performance metrics. MPBP is the amount of time required to recover the capital investment for building the HMF production section through additional profit obtained by selling HMF.

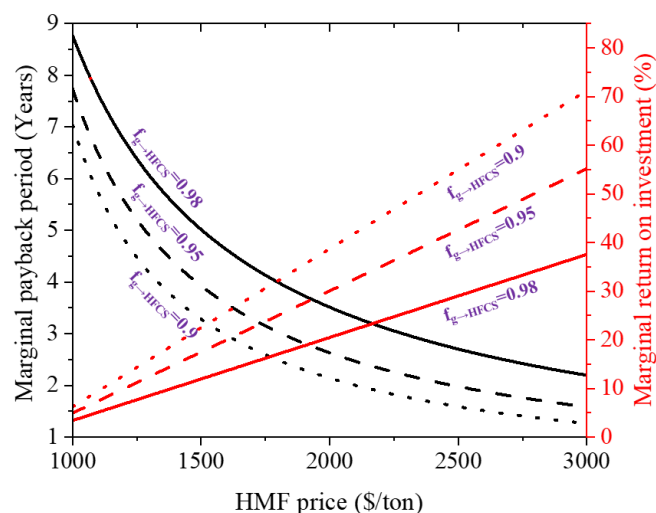


Figure 10. Economic analysis for retrofitting an existing HFCS process to produce HMF. Marginal payback period and marginal return on investment are shown as a function of HMF selling price for three different values of $f_{g \rightarrow \text{HFCS}}$.

It is defined as the ratio of TCI and sum of the difference in profits of HFCS/HMF and HFCS processes and depreciation. MROI is the additional return possible because of investing in HMF production section. It is defined as the ratio of the difference in the profits of the two processes and TCI. The fraction of glucose from starch hydrolysis section sent to syrup production section ($f_{g \rightarrow \text{HFCS}}$) and HMF price significantly affect the process economics. The effect of the two factors on MPBP and MROI are shown in Figure 10. The values of $f_{g \rightarrow \text{HFCS}}$ are chosen to be 0.9, 0.95, and 0.98 corresponding to an annual HMF production of 17.5, 9.2, and 3.5 kton, respectively. Increasing the production rate of HMF allows us to take advantages of economies of scale, resulting in lower MPBP and higher MROI.

Conclusions

We have studied a process for HMF production from glucose followed by chromatographic separation to purify HMF. Glucose feed (5.4 wt%) was dissolved in an acetone/water cosolvent at the isomerization temperature (65°C). Enzymatic isomerization of glucose produced 61.3% yield of fructose with >98% selectivity. The isomerized solution was dehydrated to a solution containing HMF, glucose, and fructose as major components (49, 32, and 7 mol%, respectively). We demonstrated that chromatography effectively separated HMF from the unreacted glucose and fructose because HMF was not adsorbed on the chromatography resin at 24°C. In contrast to HMF, fructose and glucose were adsorbed on the resin

and followed Langmuir and linear isotherm adsorption models, respectively. The thermodynamic parameters of the sugar adsorptions were determined experimentally and used in simulations to evaluate the economic potential of the process by optimizing the performance of simulated-moving-bed (SMB) separation. Techno-economic analysis indicates that the process can produce HMF at an MSP of \$1478 per ton of HMF for the base design (2000 kg·h⁻¹ of glucose feed flow rate, 8.74 kton·yr⁻¹ of HMF production). A comparison of the economics of the SMB-based process to an extraction-based process¹⁸ illustrates that the SMB-based approach is economically more favorable when the plant produces more than 8.39 kton HMF per year. We demonstrate that the proposed process can be integrated to the existing infrastructure, such as high fructose corn syrup (HFCS) production process and performed TEA to determine the process and economic conditions that make the integration economically favorable. We considered two systems that include constructing a new HFCS/HMF process and retrofitting an existing HFCS process to produce HMF. While the former system has high TCI, the latter is a particularly useful short-term strategy with low risk and low investment costs to enable the transition of emerging HMF production technology to commercial scale.

Conflicts of interest

Authors declare that there is no conflict of interest.

Acknowledgements

This material is based upon work supported in part by the Great Lakes Bioenergy Research Center, U.S. Department of Energy, Office of Science, Office of Biological and Environmental Research under Award Number DE-SC0018409 and in part by U.S. Department of Energy under Award Number DE-EE0008353. We thank Dr. Kefeng Huang for providing the model of extraction-based process. We thank Dr. Demetri Petrides at Intelligen for his help with the HFCS model.

Notes and references

- 1 Y. Román-Leshkov, C. J. Barrett, Z. Y. Liu and J. A. Dumesic, *Nature*, 2007, **447**, 982–985.
- 2 R. M. West, Z. Y. Liu, M. Peter, C. A. Gärtner and J. A. Dumesic, *J. Mol. Catal. A Chem.*, 2008, **296**, 18–27.
- 3 R. M. West, Z. Y. Liu, M. Peter and J. A. Dumesic, *ChemSusChem*, 2008, **1**, 417–424.
- 4 G. W. Huber, J. N. Chheda, C. J. Barrett and J. A. Dumesic, *Science*, 2005, **308**, 1446–1450.
- 5 J. He, K. Huang, K. J. Barnett, S. H. Krishna, D. M. Alonso, Z. J. Brentzel, S. P. Burt, T. Walker, W. F. Banholzer, C. T. Maravelias, I. Hermans, J. A. Dumesic and G. W. Huber, *Faraday Discuss.*, 2017, **202**, 247–267.
- 6 A. H. Motagamwala, W. Won, C. Sener, D. M. Alonso, C. T. Maravelias and J. A. Dumesic, *Sci. Adv.*, 2018, **4**, eaap9722.
- 7 J. Carlos Morales-Huerta, A. Martínez De Ilarduya and S. Muñoz-Guerra, *Polymer*, 2016, **87**, 148–158.

- 8 L. Sun, J. Wang, S. Mahmud, Y. Jiang, J. Zhu and X. Liu, *Eur. Polym. J.*, 2019, **118**, 642–650.
- 9 H. Chang, I. Bajaj, G. W. Huber, C. T. Maravelias and J. A. Dumesic, *Green Chem.*, 2020, **22**, 5285–5295.
- 10 T. W. Walker, A. H. Motagamwala, J. A. Dumesic and G. W. Huber, *J. Catal.*, 2019, 369, 518–525.
- 11 S. Hu, Z. Zhang, J. Song, Y. Zhou and B. Han, *Green Chem.*, 2009, **11**, 1746–1749.
- 12 J. B. Binder and R. T. Raines, *J. Am. Chem. Soc.*, 2009, **131**, 1979–1985.
- 13 J. N. Chheda, Y. Román-Leshkov and J. A. Dumesic, *Green Chem.*, 2007, **9**, 342–350.
- 14 J. N. Chheda and J. A. Dumesic, *Catal. Today*, 2007, **123**, 59–70.
- 15 T. Wang, M. W. Nolte and B. H. Shanks, *Green Chem.*, 2014, 16, 548–572.
- 16 A. Converti and M. Del Borghi, *Bioprocess Eng.*, 1997, **18**, 27–33.
- 17 Y. Román-Leshkov, M. Moliner, J. A. Labinger and M. E. Davis, *Angew. Chemie Int. Ed.*, 2010, **49**, 8954–8957.
- 18 A. H. Motagamwala, K. Huang, C. T. Maravelias and J. A. Dumesic, *Energy Environ. Sci.*, 2019, **12**, 2212–2222.
- 19 P. Y. Nikolov and V. A. Yaylayan, *J. Agric. Food Chem.*, 2011, **59**, 10104–10113.
- 20 F. K. Kazi, A. D. Patel, J. C. Serrano-Ruiz, J. A. Dumesic and R. P. Anex, *Chem. Eng. J.*, 2011, **169**, 329–338.
- 21 A. Toumi and S. Engell, *Chem. Eng. Sci.*, 2004, **59**, 3777–3792.
- 22 M. Minceva and A. E. Rodrigues, *Ind. Eng. Chem. Res.*, 2002, **41**, 3454–3461.
- 23 D. J. Gisch, C. H. Martin, C. R. Eicher, U.S. Patent, 20180001228, 2018.
- 24 K. L. Smiley, *Biotechnol. Bioeng.*, 1971, **13**, 309–317.
- 25 J. Michels, in *4.3.2 Starch Biorefinery*, ed. J. Pietzsch, Springer Verlag, 2017, pp. 91–94.
- 26 H. Chang, A. H. Motagamwala, G. W. Huber and J. A. Dumesic, *Green Chem.*, 2019, **21**, 5532–5540.
- 27 V. J. Jensen and S. Rugh, *Methods Enzymol.*, 1987, **136**, 356–370.
- 28 R. Di Cosimo, J. Mc Auliffe, A. J. Poulouse and G. Bohlmann, *Chem. Soc. Rev.*, 2013, **42**, 6437–6474.
- 29 K. M. Vilonen, A. Vuolanto, J. Jokela, M. S. A. Leisola and A. O. I. Krause, *Biotechnol. Prog.*, 2004, **20**, 1555–1560.
- 30 D. M. Alonso, J. M. R. Gallo, M. A. Mellmer, S. G. Wettstein and J. A. Dumesic, *Catal. Sci. Technol.*, 2013, **3**, 927–931.
- 31 G. Dünnebier and K. U. Klatt, *Chem. Eng. Sci.*, 2000, **55**, 373–380.
- 32 E. W. Mellow, K. E. Phillips and C. W. Myers, *Understanding Cost Growth and Performance Shortfalls in Pioneer Process Plants*, 1981.
- 33 A. Rajendran, G. Paredes and M. Mazzotti, *J. Chromatogr. A*, 2009, **1216**, 709–738.
- 34 P. Blanchard, *Technology of corn wet milling and associated processes*, Elsevier, 1992.
- 35 D. Petrides, *Corn Refinery - Modeling and Evaluation with SuperPro Designer*, 2016.
- 36 S. de Jong, R. Hoefnagels, A. Faaij, R. Slade, R. Mawhood and M. Junginger, *Biofuels, Bioprod. Biorefining*, 2015, **9**, 778–800.